

# Characterization of porous media by nuclear magnetic resonance beyond fast diffusion limit with numerical simulation

Yan Zhang\*, and Yu Zhou

State Key Laboratory of Petroleum Resources and Prospecting, China University of Petroleum, Beijing, 102249, China

**Abstract.** Nuclear magnetic resonance logging is an important formation detection technique in the petroleum industry, which is always used to detect formation pore structure and fluid identification. However, conventional nuclear magnetic resonance characterization methods assume that the formation pore medium are in fast diffusion regime. In complex formations, non-fast diffusion regimes (intermediate diffusion and slow diffusion) are also present. In the previous paper [13], a new method for characterizing porous media with non-fast diffusion regime and uniform pore size distribution by  $T_2$ - $T_2$  pulse sequence is proposed. In this research, the  $T_2$ - $T_2$  signals of periodic stacked pore models beyond fast diffusion regime are numerically simulated by the random walk algorithm, and the pore size - surface relaxivity maps are respectively inverted, the relationship between pore structure and correlation maps are discussed. The results provide theoretical foundation for characterizing pore structure beyond fast diffusion limit.

**Keywords:** NMR, Diffusion, Pore Size, Surface Relaxivity, Random Walk.

## 1 Introduction

Nuclear magnetic resonance (NMR) logging is a non-destructive technique for formation measurement. It can be used to characterize the pore structure and fluid of porous media, and can also obtain many important petrophysical parameters, such as porosity, pore size distribution, permeability, water saturation and wettability [1-5]. The NMR measurement method based on fluid spin relaxation is widely used to determine the pore size distribution of various materials based on the assumption that the fast diffusion limit is valid. This is true in many cases [6-11]

However, in complex formation, intermediate diffusion and slow diffusion ( $\kappa < 1$ ) also exists in porous media where pore size is large or surface relaxativity is strong. For example, for glass bead samples, it is found that the best fitting between relaxation time and pore size is completely different from the traditional linear relationship [12]. For porous

---

\* Corresponding author: [Zhangyannm@cup.edu.cn](mailto:Zhangyannm@cup.edu.cn)

media beyond fast diffusion regime, there is still a lack of effective means to characterize the pore structure. To solve the above problems, we proposed a new method based on the eigenmode theory and  $T_2$ - $T_2$  pulse sequence was applied to characterize the porous media [13]. Based on this research, the eigenmode method and numerical simulation method under different pore models are further studied, which lays a solid theoretical foundation for the wide application of this method. In this research,  $T_2$ - $T_2$  response signals of periodic accumulation model are simulated by random walk method, and the estimated values of pore size and surface relaxativity are obtained according to spherical pore eigenmode theory and compared with setting parameters. The relationship between spectral characteristics and pore structure under different conditions is discussed.

## 2 Eigenmode equation for relaxation

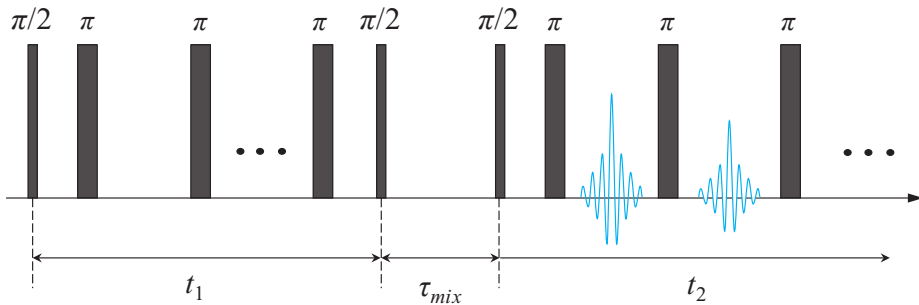


**Fig. 1.**  $T_2$ - $T_2$  pulse sequence diagram.

The NMR spin relaxation process can be described by the following equation [1-5]:

$$m(r, t) = \sum_{n=0}^{\infty} a_n \phi_n(r) e^{-t/\tau_n}, \tag{1}$$

with boundary condition:

$$D \frac{\partial}{\partial n} m(r, t) + \rho m(r, t) = 0 \tag{2}$$

where,  $a_n$  is the system index of different modes,  $m(r, t)$  is the magnetization vector of each point in the porous medium,  $r$  is the direction vector, and  $D$  is the free diffusion coefficient of the fluid in the pore,  $\partial/\partial n$  is the outward normal derivative, and  $\rho$  is the surface relaxation. The  $\phi_n$  and  $\tau_n$  are the eigenfunction and eigenvalue respectively, which satisfies the Helmholtz equation:

$$\phi_n(r)/\tau_n + D \nabla^2 \phi_n(r) = 0, \tag{3}$$

The NMR relaxation signal of the pulse sequence in Fig. 1 can be expressed as:

$$M(t_1, t_2) = \sum_{n,m,p} \langle 1 | \phi_{2,n} \rangle \langle \phi_{2,n} | \phi_{1,p} \rangle \langle \phi_{1,p} | \phi_{2,m} \rangle \langle \phi_{2,m} | 1 \rangle \times \exp(-t_1/\tau_{2,n} - \tau_{mix}/\tau_{1,p} - t_2/\tau_{2,m}) \tag{4}$$

where  $t_1$  is the duration of first CPMG sequence and  $t_2$  is the duration of second CPMG acquisition sequence,  $\tau_{mix}$  is mixing time,  $\langle \cdot | \cdot \rangle$  is the Dirac symbol (also known as "bra ket symbol"),  $|1\rangle$  indicates that the uniform magnetization state of the whole system is equal to 1, and its calculation method can be defined as:

$$\langle \phi | \phi \rangle = \int \phi^* \phi dv, \tag{5}$$

where  $\phi^*$  is an complex conjugate function of  $\phi$ . In order to reduce the effect of longitudinal surface relaxation,  $\tau_{mix}$  is set to 0, equation (4) can be simplified as:

$$M(t_1, t_2) = M(0) \sum_n \langle 1 | \phi_{2,n} \rangle^2 \exp(-t_1/\tau_{2,n} - t_2/\tau_{2,n}), \tag{6}$$

The above equation can be used to inverse the  $T_2 - T_2$  data to obtain the pore size and surface relaxativity correlation map beyond fast diffusion limit [14].

### 3 Numerical simulation

Monte Carlo random walk algorithm is used to simulate NMR response. The fluid in the pore is set as water, and the diffusion coefficient  $D$  is  $2.5 \times 10^{-9} \text{m}^2/\text{s}$ . In order to increase the stability of the simulation and reflect the relaxation characteristics of the pore surface better, the number of random particles is set to 10000. In order to improve the simulation efficiency, the parallel algorithm of MATLAB is used to greatly shorten the time required in the simulation. The periodic accumulation model is selected, as shown in Figure 2, the gray stacked spheres represent solid skeleton particles, with 1000 spherical particles and a porosity of 47.6%.

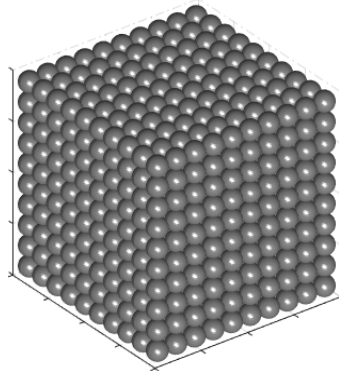


**Fig. 2.** The periodic stacked pore model.

The pore size  $a$  can be approximately equal to the radius of spherical particles and four pore models are selected: pore I ( $a = 100 \mu\text{m}$ ,  $\rho = 25 \mu\text{m/s}$ ), Pore II ( $a = 200 \mu\text{m}$ ,  $\rho = 50 \mu\text{m/s}$ ), pore III ( $a = 250 \mu\text{m}$ ,  $\rho = 100 \mu\text{m/s}$ ), Pore IV ( $a = 400 \mu\text{m}$ ,  $\rho = 100 \mu\text{m/s}$ ) and the corresponding  $\kappa$  are: 1, 4, 10 and 16. The corresponding initial  $T_2 - T_2$  signals are simulated by random walk algorithm, and the pore size surface relaxativity correlation spectra with different  $k$  under two signal-to-noise ratios are obtained by non negative least square inversion method, as shown in Fig. 3:

The approximate range of pore size and surface relaxativity can be estimated from these correlation spectra in the above figure: pore model I ( $\kappa = 1$ ,  $a = 100 \mu\text{m}$ ,  $\rho = 25 \mu\text{m/s}$ ), as shown in Fig. 3a-b, the spectral peak positions under the two signal-to-noise ratios are

roughly the same, in which the pore size is about 80-110  $\mu\text{m}$  and the surface relaxativity is 20-40  $\mu\text{m}/\text{s}$ . The estimated value range is near the set value of pore model I. Pore model II ( $\kappa = 4$ ,  $a = 200 \mu\text{m}$ ,  $\rho = 50 \mu\text{m}/\text{s}$ ) are shown in Fig. 3c-d. The estimated values (pore size: 180-210  $\mu\text{m}$  and  $\rho$ : 30-70  $\mu\text{m}/\text{s}$ ) agree well with the the set value. The third pore model ( $\kappa = 10$ ,  $a = 250 \mu\text{m}$ ,  $\rho = 100 \mu\text{m}/\text{s}$ ) are shown in Fig. 3e-f. The pore size is about 280-200  $\mu\text{m}$  and the surface relaxativity is 70-150  $\mu\text{m}/\text{s}$ , the characterization result is good. The fourth pore model ( $\kappa = 16$ ,  $a = 400 \mu\text{m}$ ,  $\rho = 100 \mu\text{m}/\text{s}$ ) are shown in Fig. 3g-h. The spectrum is split, in which the pore size of the main peak is about 240-300  $\mu\text{m}$  and the surface relaxativity is 30-100  $\mu\text{m}/\text{s}$ . The characterization results are distorted.

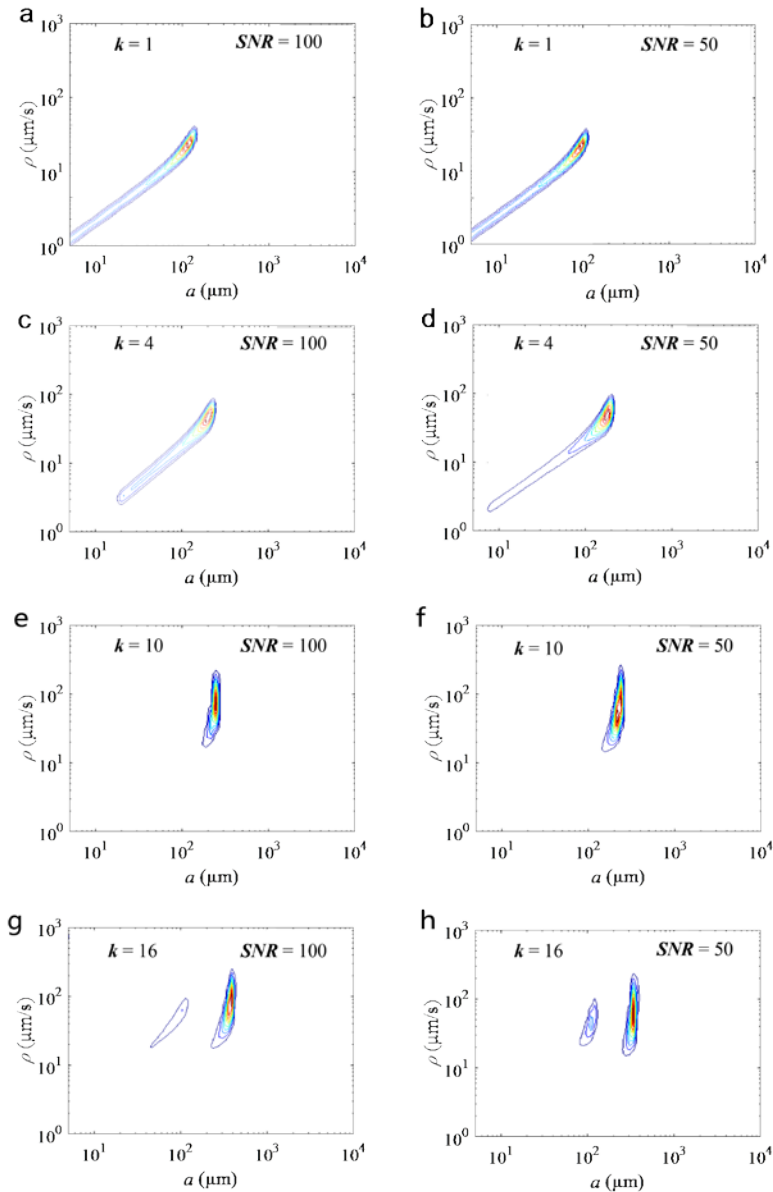


**Fig. 3.**  $a$ - $\rho$  correlation maps of periodic stacked pores.

To sum up, for the periodic accumulation pore model, the pore size distribution is relatively uniform. When the pore model is in the intermediate diffusion condition ( $1 < \kappa < 10$ ), the inversion effect is good in both two signal-to-noise ratios. Therefore, this method can effectively characterize the periodic accumulation pore model beyond fast diffusion conditions.

## 4 Conclusion

Based on the numerical simulation, the method of  $T_2$ - $T_2$  sequence to characterize the structure of porous media beyond fast diffusion conditions is examined. The correlation between pore size and surface relaxativity of corresponding porous media is obtained by inversion. The results are consistent with the preset pore parameters and verified by experiments. The main conclusions are as follows:

(1) The numerical simulation shows that the estimated range of pore size and surface relaxativity agree with the set value in different diffusion regime.

(2) This method is most suitable for intermediate diffusion conditions ( $1 < \kappa < 10$ ). The estimated values of pore size and surface relaxativity are more accurate, and the distribution range of pore size is smaller than that of surface relaxativity. When  $\kappa$  is too large (slow diffusion condition), it is difficult to obtain surface relaxativity and the spectral are distorted.

Financial Supported by the National Natural Science Foundation of China (Grant No. 41804109) and Science Foundation of China University of Petroleum, Beijing (Grant No. 2462020YXZZ007) is gratefully acknowledged.

## Reference

1. P. T. Callaghan, Oxford University Press (2011).
2. M. H. Cohen, K. S. Mendelson, *Journal of Applied Physics*, 53(2): 1127-1135 (1982).
3. L. J. Zielinski, Y. Q. Song, S. Ryu, et al, *The Journal of Chemical Physics*, 117(11): 5361-5365 (2002).
4. K. R. Brownstein, C. E. Tarr, *Physical Review A*, 19(6): 2446 (1979).
5. K. R. Mccall, D. L. Johnson, R. A. Guyer, *Physical Review B*, 44(14): 7344 (1991).
6. D. S. Grebenkov, *Reviews of Modern Physics*, 79(3): 1077 (2007).
7. C. H. Arns, A. P. Sheppard, M. Saadatfar, et al., *SPWLA 47th Annual Logging Symposium. Society of Petrophysicists and Well-Log Analysts* (2006).
8. A. Valfouskaya, M. P. Adler, J. F. Thovert, et al., *Journal of Colloid and Interface science*, 295(1): 188-201 (2006).
9. Y. Q. Song, L. Venkataramanan, M. D. Hürlimann, et al., *Journal of Magnetic Resonance*, 154(2): 261-268 (2002).
10. M. D. Hürlimann, L. Venkataramanan, *Journal of Magnetic Resonance*, 157(1): 31-42 (2002).
11. L. Venkataramanan, Y. Q. Song, M. D. Hürlimann, *IEEE Transactions on Signal Processing*, 50(5): 1017-1026 (2002).
12. K. Keating, R. Knight, *Geophysics*, 77(5): E365-E377 (2012).
13. Z. Yu, Y. Zhang, L. Xiao, G. Liao, *Magnetic Resonance Imaging*, 56: 19-23 (2019).